Edge-carboxylated graphene nanoflakes from nitric acid oxidised arc-discharge material

Christoph G. Salzmann,*[a] Valeria Nicolosi[b] and Malcolm L. H. Green[a]

Received 16th July 2009, Accepted 10th September 2009
First published as an Advance Article on the web 30th October 2009
DOI: 10.1039/b914288f

Graphene nanoflakes (GNFs) with average diameters of ~30 nm have been prepared by a single-step oxidation procedure using single-wall carbon nanotube arc-discharge material and nitric acid. The GNFs are predominately single sheets containing a small number of internal defects. The edges are decorated with primarily carboxylic acid groups which allow facile chemical functionalisation and cross-linking of the fragments using multivalent cations.

Introduction

Two-dimensional carbon materials have attracted considerable interest since the discovery that a single sheet of sp^2 carbon, graphene, can be isolated.[1,2] Graphene displays a variety of remarkable physical properties such as high mobility of charge carriers,[3] mechanical stability[4] and thermal conductivity.[5]

The original preparation procedure for graphene relied on micromechanical exfoliation of graphite which yielded relatively small amounts of sample.[2] Graphene layers have also been grown on metal substrates by using chemical vapour deposition techniques.[6] Very recently, graphene nanoribbons have been prepared by chemically 'unzipping' carbon nanotubes or by plasma etching carbon nanotubes.[7,8] Most chemical procedures for the bulk production of graphene rely on the oxidation of graphite to graphite oxide in a first step, which requires very aggressive oxidation conditions, and subsequent chemical reduction by using, for example, hydrazine.[9–11]

For studies on the physical properties of graphene it is often advantageous to have as large sheets as possible. Regarding the chemical functionalisation, however, it may be more useful to have smaller fragment sizes which should disperse more readily in the reaction media. Furthermore, the increased relative number of functional groups at the edges of smaller fragments should facilitate the structural characterisation of the product materials.

Here we show that predominately single-sheet graphene nanoflakes (GNFs) with average lateral diameters of about 30 nm can be produced in a single step by oxidation of single-wall carbon nanotube arc-discharge material with nitric acid. The presence and location of functional groups have been investigated as well as the chemical reactivity and dispersibility in water and organic solvents.

[a]*Department of Chemistry, Inorganic Chemistry Laboratory, University of Oxford, South Parks Road, Oxford, UK OX1 3QR. E-mail: christoph.salzmann@chem.ox.ac.uk; Fax: +44 (0)1865 2 72690; Tel: +44 (0)1865 2 72645*
[b]*Department of Materials, University of Oxford, Parks Road, Oxford, UK OX1 3PH*

Experimental

Preparation and purification of materials

Single-wall carbon nanotube (SWCNT) arc-discharge material (Carbolex AP grade or in-house produced material) containing a Ni/Y catalyst[12] was subjected to a microwave treatment in 16% hydrochloric acid[13] followed by refluxing for 24 h. In separate experiments, 500 mg of graphite (Aldrich, 282863), carbon nanopowder (Aldrich, 633100), catalyst free arc-discharge multi-wall carbon nanotube material (Aldrich, 412988) and the HCl treated SWCNT arc-discharge material were refluxed in 500 mL 9 M nitric acid for 24 h. The filtrate of the SWCNT arc-discharge material was then neutralised under external ice cooling and vigorous stirring by slowly adding sodium hydroxide pellets. The formation of a dark brown precipitate was observed which was isolated by filtration and stirred in 5 mL of a 0.2 M potassium cyanide solution for 24 h. After filtration, the material was washed with KCN solution on the filter membrane, again stirred in KCN solution and recovered by filtration. The material was then combined with 50 mL of deionised water and carefully neutralised by adding drops of 1 M hydrochloric acid under stirring. After filtration, the material on the filter membrane was washed with an excess of water and dried in a desiccator under vacuum (dry mass = 80 mg). For further purification, some of the material was dispersed in 1 M formic acid, dialysed against 1 M formic acid solution and then against Millipore deionised water (10 mL Spectra/Por Float-A-Lyzer MWCO 2000). A dark brown powder was obtained after lyophilisation of the dialysed dispersion.

Amidation reaction

5 mg of the purified material were dispersed in a mixture of 20 mL tetrahydrofuran (THF) and 3 mL oxalyl chloride, and heated at 40 °C under dinitrogen atmosphere for 18 h. THF and oxalyl chloride were then evaporated under vacuum, and the residue was combined with 3 mL dry ethylenediamine and 20 mL dry THF. Upon stirring at 40 °C for 4 h under dinitrogen precipitation was observed, and ethylenediamine and THF were removed under vacuum at 50 °C. The residue was stirred in water overnight, washed with an excess of water on a filter membrane and then dried in a desiccator.

Sample characterisations

Optical absorbance spectra were recorded in quartz cuvettes (10 mm light path length) on a GBC spectrometer (Cintra 10). X-Ray photoelectron spectroscopy was performed in an ion pumped UHV chamber equipped with a VG nine channel CLAM4 electron energy analyser using 300 W unmonochromated Mg Kα X-ray radiation. The analyser was operated at constant pass energy of 100 eV for wide scans and 20 eV for detailed scans. ATR FT-IR spectra were obtained using a Nicolet 6700 spectrometer equipped with a Golden Gate ATR cell. Raman spectra were recorded on a Jobin Yvon Labram spectrometer using a HeNe laser (632.8 nm, 2 mW). ^{13}C NMR spectra were collected using a Varian CMX MSL 400 MHz solid state NMR spectrometer. A Digital Instruments Multimode Nanoscope Scanning Probe Microscope was used for scanning tunneling microscopy (STM) and atomic force microscopy (AFM) in tapping mode. For STM and AFM analysis, the sample dispersions were dropped onto freshly cleaved 'highly oriented pyrolytic graphite' (HOPG) using a Laurell Technologies WS-400 spin-coater (8000 rpm). The cleanliness of the substrate was ensured beforehand by using STM or AFM. For TEM analysis, dispersions of the samples in water or ethanol were dropped onto a lacey carbon support grid (500 mesh). Transmission electron microscopy images were taken using a JEM-3000F FEGTEM (300 kV) or the Oxford-Jeol JEM-2200MCO double aberration corrected microscope (80 kV). Electron diffraction patterns were recorded on the JEM-3000F.

Results and discussion

A variety of carbon materials were subjected to an oxidative treatment by refluxing in 9 M nitric acid. In the case of graphite, carbon nanopowder and the arc-discharge multi-wall carbon nanotube material colourless filtrates were obtained. The reaction of the single-wall carbon nanotube (SWCNT) arc-discharge material with nitric acid on the other hand produced a dark orange filtrate (*cf.* Fig. 1).

After careful neutralisation of the filtrate with sodium hydroxide pellets a voluminous, dark brown precipitate was obtained which was isolated by filtration. Elemental analysis using X-ray photoelectron spectroscopy (XPS) showed that the sample contained carbon as well as oxygen, nickel(II) and yttrium(III) (*cf.* Fig. 2a, spectrum (1)). The nickel impurity was removed quantitatively by treatment with potassium cyanide solution (*cf.* spectrum (2)). Further purification using dialysis led to almost complete removal of yttrium from the sample (*cf.* spectrum (3)). After lyophilisation of the dialysed dispersion, the sample was dispersible in water across the entire pH range as well as in other polar solvents such as tetrahydrofuran, dimethylformamide and methanol.

The high-resolution XP spectrum of the C 1s region of the purified sample showed that a large portion of the carbon atoms were unoxidised after the nitric acid treatment as indicated by the binding energy of 284.7 eV of the main peak (*cf.* spectrum (1) in Fig. 2b). This illustrates the relatively 'weak' oxidation power of 9 M nitric acid compared to, for example, the conditions necessary for the formation of graphite oxide from graphite (*e.g.* $NaClO_3$–fuming HNO_3) after which the peak around 284.7 eV was either greatly diminished or not present anymore (*cf.* Fig. 8 in ref. 14). The weak peak at 286.7 eV is attributed to C(I) or C(II) species such as alcohols, epoxides, aldehydes or ketones, and the peak at 288.4 eV is commonly assigned to C(III) species such as carboxylic acids, anhydrides or lactones.[15,16] After heating the sample at 850 °C under argon the peaks at higher binding energies disappeared, and the spectrum typical for graphitic carbon with a peak centred at 284.9 eV and tailing on the high-energy side was obtained (*cf.* spectrum (2)).[15,17] Peak asymmetry, which is difficult to fit, may also present for the main peak in spectrum (1), and the peak areas of the C(I) or C(II) species in particular but also of the C(III) carbon species may therefore be smaller than the values obtained from peak fitting using

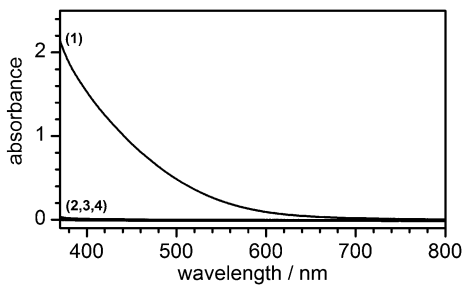

Fig. 1 Optical absorbance spectra of the filtrates obtained after the treatment of (1) arc-discharge single-wall carbon nanotube material, (2) graphite, (3) carbon nanopowder and (4) arc-discharge multi-wall carbon nanotube material in 9 M nitric acid for 24 h at 100 °C. The curves of filtrates (2–4) overlap. Nitric acid absorbs strongly below ~370 nm and this spectral range is not shown.

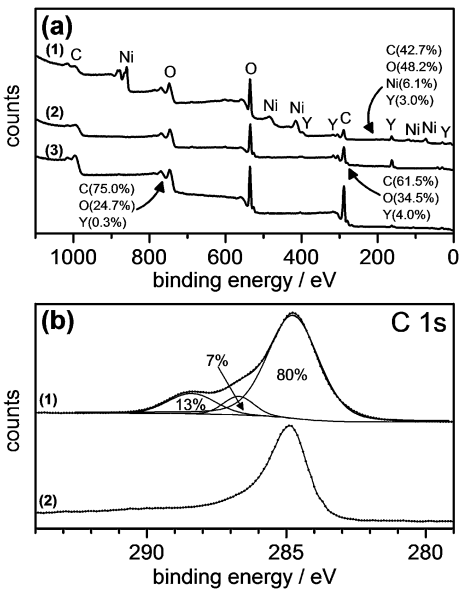

Fig. 2 (a) X-Ray photoelectron spectroscopy survey scans of the material (1) after precipitation, (2) after treatment with KCN solution and (3) after dialysis. The elemental composition of the samples is given in atom percent for each spectrum. (b) High-resolution spectra of the C 1s region of the purified sample (1) before and (2) after annealing at 850 °C under argon. Fitted peaks and relative area percentages are shown for spectrum (1).

symmetric peaks. Consequently, the peak area of graphitic carbon is expected to be slightly higher than 80%.

The FT-IR spectrum of the purified sample (*cf.* spectrum (1) in Fig. 3a) shows a broad peak centred at 1714 cm^{-1} which is about the ν(C=O) stretching frequency expected for carboxylic acid groups (1700–1725 cm^{-1}) or lactones (~1735 cm^{-1}).[18] Anhydrides typically show higher stretching frequencies. For example, 1779 cm^{-1} is observed for 1,4,5,8-naphthalenetetracarboxylic dianhydride.[19] Anhydride groups are therefore probably not present in the sample, at least not in significant quantities. The lower frequency peak at 1600 cm^{-1} is assigned to aromatic ν(C=C) stretching modes. After annealing the sample at 850 °C under argon the ν(C=O) peak disappears completely as a consequence of decarboxylation (*cf.* spectrum (2)). The purified sample was also reacted with oxalyl chloride and then with ethylenediamine (*cf.* Experimental). Carboxylic acid groups (COOH) are expected to form amides under these reaction conditions, and the spectrum of the sample after the reactions showed that the ν(C=O) mode had shifted to 1652 cm^{-1} which is in accordance with the formation of an amide (*cf.* spectrum (3)).[18] XPS analysis also confirmed the presence of nitrogen in the sample after the reactions (not shown). From this it is concluded that a substantial fraction of C(III) species present in the sample are carboxylic acid groups.

Raman spectroscopy showed the presence of sp^2 carbon in all samples as indicated by the G-band (graphitic band) at ~1590 cm^{-1} and the D-band (disorder band) at ~1360 cm^{-1} (*cf.* Fig. 3b). The high-temperature annealing under argon shifted the D-band to ~1330 cm^{-1}. The D-band in carbon materials is generally associated with the presence of 'disorder' such as defects or simply nanoscale dimensions.

The ^{13}C NMR spectrum of the purified material shows two broad peaks centred at about 134 and 173 ppm (*cf.* Fig. 3c). In line with previous studies the 134 ppm peak is assigned to sp^2 carbon.[14,20,21] Peaks in the 170 ppm region have been observed before for oxidised graphite materials, however, with very weak intensities.[14,21] A chemical shift of 173 ppm is within the range expected for carboxylic acid groups.[22] In the case of graphite oxide it has been stated that "carboxylic acid groups, which are located at the edges of the basal plane, are too few for ^{13}C NMR detection."[23] The relatively strong intensity of the 173 ppm peak therefore suggests that a high number of oxidised edge sites are present in the sample.

The spectroscopic data lead to the conclusion that the sample consists of carboxylated graphene nanoflakes (GNFs) similar to the one shown schematically in Fig. 3d. Scanning tunneling microscopy (STM) (*cf.* Fig. 4a) and transmission electron microscopy (TEM) (*cf.* Fig. 5a) showed, however, that the fragments were much larger than the one depicted in Fig. 3d. The

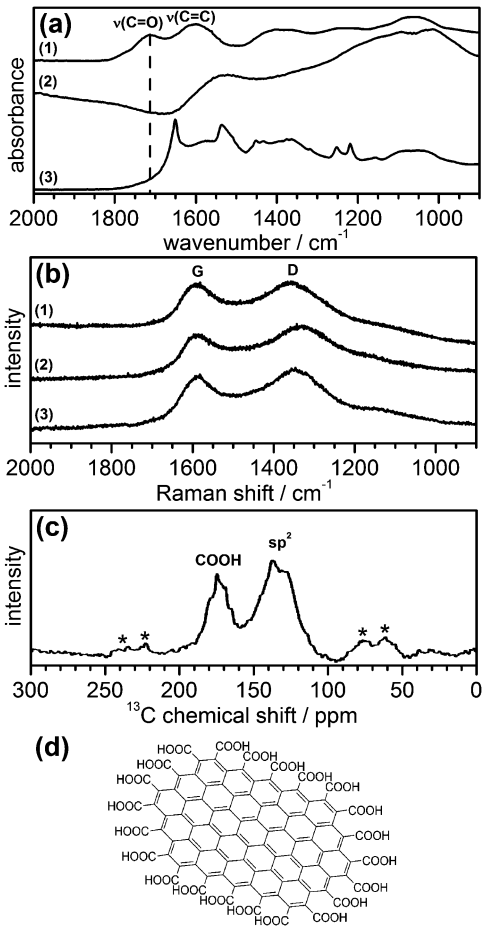

Fig. 3 (a) FT-IR spectra (1) of the purified sample, (2) after annealing at 850 °C under argon and (3) after the amidation reaction. (b) Raman spectra of the same samples. (c) Solid state ^{13}C NMR spectrum of the purified sample. The asterisks indicate spinning side bands. (d) Idealised chemical structure of a small edge-carboxylated graphene nanoflake.

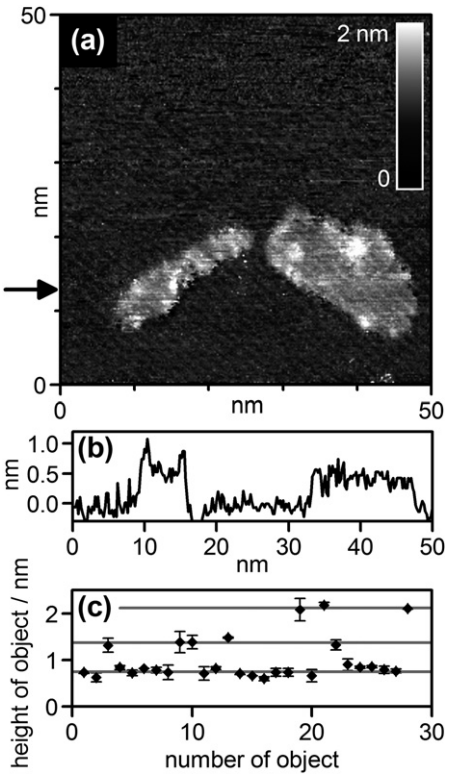

Fig. 4 (a) Scanning tunneling microscopy image of two graphene nanoflakes. (b) Height profile along the direction indicated in (a). (c) Height analysis of the GNFs. Horizontal lines indicate the average step heights for single, double and triple layer fragments.

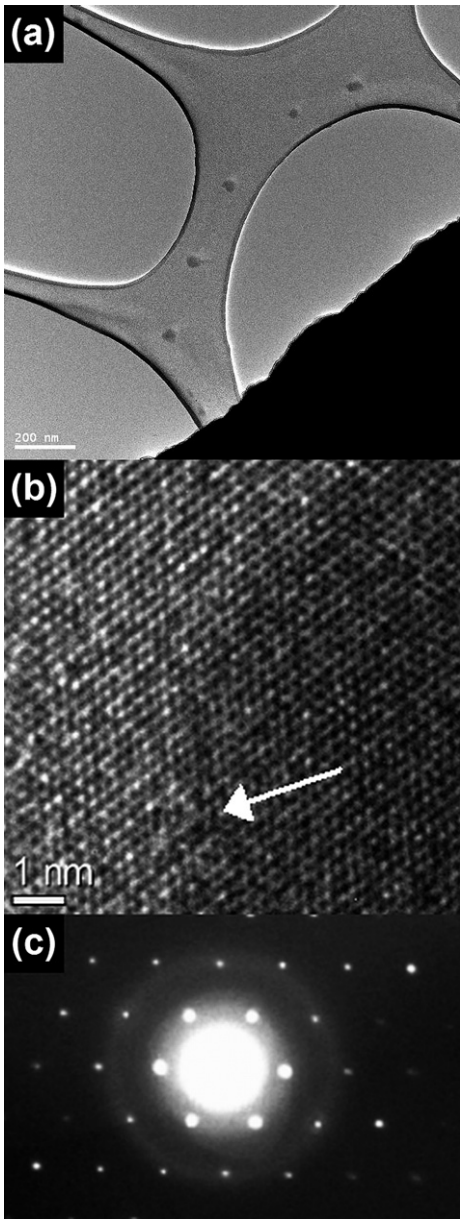

Fig. 5 (a) Transmission electron microscopy image of graphene nanoflakes deposited onto a lacey carbon support grid. (b) High-resolution image of the interior of a graphene nanoflake. The arrow indicates a structural defect. (c) Electron diffraction pattern of the interior of a GNF.

average lateral length, measured along the longest distance across the fragments, is 30 ± 9 nm as determined from the STM data. STM step-height analysis showed that the largest fraction of the fragments (~70%) is about 0.7 nm in height (*cf.* Fig. 4b and c). Only a few fragments had about twice or three times this step-height suggesting that the majority of the fragments consist of single layer sheets and that only a few double and triple layered GNFs are present in the sample.

The existence of single sheets was also shown by using normal-incidence selected area electron diffraction measurements which showed the pattern expected for a single sheet of graphene with the innermost reflections being the most intensive ones (*cf.* Fig. 5c).[24,25] High-resolution TEM of the GNFs showed the regular hexagonal structure expected for graphene. Only a small number of internal defect 'islands', such as the one indicated by the arrow in Fig. 5b, could be found within the graphene sheets.

The binding of COOH groups onto pristine and defective graphene has been investigated computationally.[26,27] The defects observed here are, however, larger than the ones investigated computationally and contain therefore most likely several functional groups—assuming that the defects do not form due to the exposure of the sample to the electron beam. In general, the mechanism for the formation of internally carboxylated graphene would have to involve the transformation of a carbon atom already existing within the graphene sheet to a COOH group. The adsorption of COOH onto pristine or defective graphene seems chemically unlikely.

The small number of defects within the sheets suggests that the majority of the COOH groups are decorating the edges of the sheets as shown schematically in Fig. 3d. In order to investigate this further, 25 μL of a 1 mg mL^{-1} $CaCl_2$ solution were added to 1 mL of a 1 mg mL^{-1} GNF dispersion resulting in a final Ca^{2+} concentration of ~0.2 mmol L^{-1}. The divalent Ca^{2+} cations are expected to be complexated by the carboxylic acid groups at neutral pH,[28] thereby cross-linking GNFs together. Indeed, complete precipitation was observed within about 30 min. Similar cross-linking using Mg^{2+} or Ca^{2+} cations has in fact been shown to improve the mechanical properties of graphene oxide papers.[29]

After precipitation, the sample vial was subjected to ultrasonication using a bath sonicator for about 3 min which led to complete redispersion of the sample. A drop of the dispersion was then quickly dropped onto a freshly cleaved, rotating HOPG substrate in a spin-coater. Analysing the surface using atomic force microscopy (AFM) revealed that the GNFs were aggregated 'edge-to-edge' and formed agglomerates of two, three or four fragments under these conditions. Fig. 6 shows such an agglomerate which consists of three cross-linked GNFs. Apart from GNF agglomerates, it was also found that the GNFs

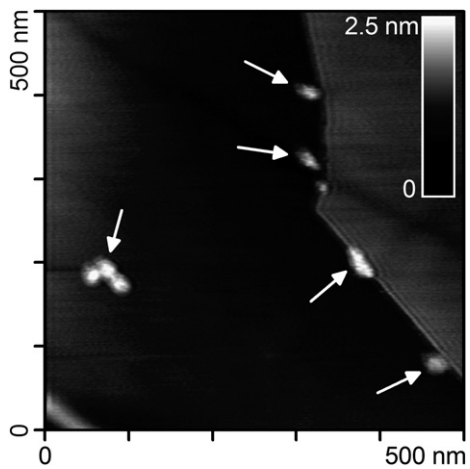

Fig. 6 Atomic force microscopy image of a freshly ultrasonicated graphene nanoflake dispersion containing Ca^{2+} deposited onto HOPG. Arrows indicate the aggregation of graphene nanoflakes with each other or at a step defect.

decorate the step defects of HOPG suggesting that the steps may also be terminated by some functional groups, such as COOH groups, which can bind Ca^{2+} ions. The fact that the fragments join together 'edge-to-edge' and do not 'pile up' strongly suggests that the majority of the COOH groups are decorating the edges of the GNFs.

GNF dispersions were also found to precipitate upon addition of YCl_3 solution, and this is most likely the reason why precipitation is observed upon neutralising the filtrate of the initial nitric acid solution in which some yttrium(III) is present from the Ni/Y catalyst (*cf.* Experimental and Fig. 2a). This illustrates how the presence of small amounts of multivalent cations can compromise the dispersion properties of carbon materials containing carboxylic acid groups.

Subjecting the SWCNT material to a second treatment with nitric acid led again to the formation of a dark orange filtrate. However, in order to precipitate the material upon neutralisation, it is necessary to add some $CaCl_2$ or YCl_3 solution before neutralisation.

Arc-discharge SWCNT materials are well known to contain considerable fractions of 'amorphous carbon'.[30,31] The fact that the GNFs can be isolated after the oxidative treatment of the arc-discharge material using nitric acid suggests that graphitic or graphenic fragments of similar dimensions may already be present in the as-made material. In fact, detailed TEM analysis of the arc-discharge material before the nitric acid treatment showed the existence of graphenic regions within the 'amorphous carbon' (indicated by the arrow in Fig. 7a). The graphenic fragments are perhaps interconnected by carbon species which can be oxidised by nitric acid which then liberates the GNFs. It has been shown previously that as-made SWCNTs are quite resilient towards oxidation with 9 M nitric acid.[32] The dimensions of the GNFs make it seem unlikely that the fragments originate from the decomposition reaction of SWCNTs. It was also found that some of the GNFs adsorb onto the SWCNTs, and they were identified as the main 'carriers' of the COOH functionality after treatment of as-made SWCNT materials with nitric acid.[32–34] Fig. 7b shows a TEM image of the SWCNT material after the nitric acid treatment. Very recent work has shown that the arc-discharge process can be optimised towards the formation of 2–4 layer graphene in the presence of hydrogen.[35]

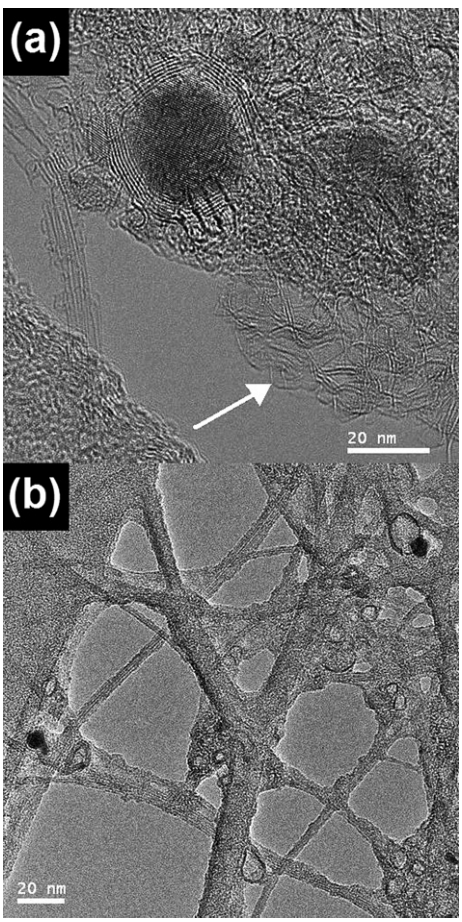

Fig. 7 Transmission electron microscopy images of the single-wall carbon nanotube (SWCNT) arc-discharge material (a) before and (b) after the treatment with nitric acid (*cf.* Experimental). The arrow in (a) indicates a region of graphenic carbon.

The oxidative treatment of the multi-wall carbon nanotube arc-discharge material with nitric acid did not lead to the formation of GNFs as can be seen from the optical absorbance spectrum of the filtrate shown in Fig. 1. The multi-wall material does not contain a Ni/Y catalyst which shows that the presence of the metal catalyst is not only important for forming SWCNTs but also the graphenic fragments. It seems possible that the fragments form in a side-reaction to the SWCNT formation. Unlike single-wall carbon nanotubes, which can grow up to lengths of several micrometres, the growth process of the fragments seems to stop much earlier as reflected by the smaller dimensions of the GNFs.

Conclusions

Flakes of graphitic carbon with average lateral diameters of ~30 nm have been prepared. The graphene nanoflakes (GNFs) consist predominantly of single sheets and show a small number of defects within the sheets. Unlike the preparation of chemically modified graphene from graphite which, in most cases, requires the oxidation of graphite to graphite oxide first, the preparation of GNFs takes place in a single oxidation step using arc-discharge single-wall carbon nanotube material and nitric acid. The edges of the graphene fragments are decorated with mainly carboxylic acid groups (COOH). The GNFs show excellent dispersion properties in water and other polar solvents in the absence of multivalent cations, and the COOH groups can be easily functionalised using carboxylate chemistry. The dispersion and chemical reactivity properties of this material make them ideally suited for further studies into the chemical functionalisation of oxidised graphene edges. Applications in which the GNFs act as a 'junction box' mediating electron transfer between redox-active groups linked to the edges of the GNFs are anticipated.

Acknowledgements

We thank Dr N. Rees for recording NMR spectra, Dr R. Jacobs for help with scanning tunneling microscopy, Dr A. Crossley for help with X-ray photoelectron spectroscopy, BegbrokeNano

for access to instruments, and Dr J. M. Brown, Dr K. A. Vincent and Dr J. A. Raskatov for discussions. We are grateful to the Austrian Academy of Sciences for an APART grant (C.G.S.) and the EPSRC for granting access to the NCESS facility (EP/E025722/1).

Notes and references

1 K. S. Novoselov, A. K. Geim, S. V. Morozov, D. Jiang, Y. Zhang, S. V. Dubonos, I. V. Grigorieva and A. A. Firsov, *Science*, 2004, **306**, 666–669.
2 K. S. Novoselov, D. Jiang, F. Schedin, T. J. Booth, V. V. Khotkevich, S. V. Morozov and A. K. Geim, *Proc. Natl. Acad. Sci. U. S. A.*, 2005, **102**, 10451–10453.
3 K. I. Bolotin, K. J. Sikes, Z. Jiang, M. Klima, G. Fudenberg, J. Hone, P. Kim and H. L. Stormer, *Solid State Commun.*, 2008, **146**, 351–355.
4 C. Lee, X. Wei, J. W. Kysar and J. Hone, *Science*, 2008, **321**, 385–388.
5 A. A. Balandin, S. Ghosh, W. Bao, I. Calizo, D. Teweldebrhan, F. Miao and C. N. Lau, *Nano Lett.*, 2008, **8**, 902–907.
6 M. Eizenberg and J. M. Blakely, *Surf. Sci.*, 1970, **82**, 228–236.
7 L. Jiao, L. Zhang, X. Wang, G. Diankov and H. Dai, *Nature*, 2009, **458**, 877–880.
8 D. V. Kosynkin, A. L. Higginbotham, A. Sinitskii, J. R. Lomeda, A. Dimiev, B. K. Price and J. M. Tour, *Nature*, 2009, **458**, 872–877.
9 S. Stankovich, R. D. Piner, X. Chen, N. Wu, S. T. Nguyen and R. S. Ruoff, *J. Mater. Chem.*, 2006, **16**, 155–158.
10 D. Li, M. B. Muller, S. Gilje, R. B. Kaner and G. G. Wallace, *Nat. Nanotechnol.*, 2008, **3**, 101–105.
11 S. Park and R. S. Ruoff, *Nat. Nanotechnol.*, 2009, **4**, 217–224.
12 C. Journet, W. K. Maser, P. Bernier, A. Loiseau, M. L. de la Chapelle, S. Lefrant, P. Deniard, R. Lee and J. E. Fischer, *Nature*, 1997, **388**, 756–758.
13 A. R. Harutyunyan, B. Pradhan, J. Chang, G. Chen and P. C. Eklund, *J. Phys. Chem. B*, 2002, **106**, 8671–8675.
14 T. Szabo, O. Berkesi, P. Forgo, K. Josepovits, Y. Sanakis, D. Petridis and I. Dekany, *Chem. Mater.*, 2006, **18**, 2740–2749.
15 A. Jung, R. Graupner, L. Ley and A. Hirsch, *Phys. Status Solidi B*, 2006, **243**, 3217–3220.
16 S. Kundu, Y. Wang, W. Xia and M. Muhler, *J. Phys. Chem. C*, 2008, **112**, 16869–16878.
17 H. Estrade-Szwarckopf, *Carbon*, 2004, **42**, 1713–1721.
18 J. Coates, in *Encyclopedia of Analytical Chemistry*, ed. R. A. Meyers, John Wiley & Sons Ltd., Chichester, 2000, pp. 10815–10837.
19 Y. Ofir, A. Zelichenok and S. Yitzchaik, *J. Mater. Chem.*, 2006, **16**, 2142–2149.
20 A. Lerf, H. He, M. Forster and J. Klinowski, *J. Phys. Chem. B*, 1998, **102**, 4477–4482.
21 W. Cai, R. D. Piner, F. J. Stadermann, S. Park, M. A. Shaibat, Y. Ishii, D. Yang, A. Velamakanni, S. J. An, M. Stoller, J. An, D. Chen and R. S. Ruoff, *Science*, 2008, **321**, 1815–1817.
22 E. Breitmaier and G. Bauer, *^{13}C NMR Spectroscopy*, Harwood Academic Publishers, Chur, 1984.
23 X. Fan, W. Peng, Y. Li, X. Li, S. Wang, G. Zhang and F. Zhang, *Adv. Mater.*, 2008, **20**, 4490–4493.
24 J. C. Meyer, A. K. Geim, M. I. Katsnelson, K. S. Novoselov, D. Obergfell, S. Roth, C. Girit and A. Zettl, *Solid State Commun.*, 2007, **143**, 101–109.
25 Y. Hernandez, V. Nicolosi, M. Lotya, F. M. Blighe, Z. Sun, S. De, I. T. McGovern, B. Holland, M. Byrne, Y. K. Gun'ko, J. J. Boland, P. Niraj, G. Duesberg, S. Krishnamurthy, R. Goodhue, J. Hutchison, V. Scardaci, A. C. Ferrari and J. N. Coleman, *Nat. Nanotechnol.*, 2008, **3**, 563–568.
26 F. Ouyang, B. Huang, Z. Li, J. Xiao, H. Wang and H. Xu, *J. Phys. Chem. C*, 2008, **112**, 12003–11207.
27 N. Al-Aqtash and I. Vasiliev, *J. Phys. Chem. C*, 2009, **113**(30), 12970–12975.
28 H. Bazin, A. Bouchu, G. Descotes and M. Petit-Ramel, *Can. J. Chem.*, 1995, **73**, 1338–1347.
29 S. Park, K.-S. Lee, G. Bozoklu, W. Cai, S. T. Nguyen and R. S. Ruoff, *ACS Nano*, 2008, **2**, 572–578.
30 M. E. Itkis, D. E. Perea, R. Jung, S. Niyogi and R. C. Haddon, *J. Am. Chem. Soc.*, 2005, **127**, 3439–3448.
31 M. E. Itkis, D. E. Perea, S. M. Niyogi, S. M. Rickard, M. A. Hamon, H. Hu, B. Zhao and R. C. Haddon, *Nano Lett.*, 2003, **3**, 309–314.
32 C. G. Salzmann, S. A. Llewellyn, G. Tobias, M. A. H. Ward, Y. Huh and M. L. H. Green, *Adv. Mater.*, 2007, **19**, 883–887.
33 H. Yu, Y. Jin, F. Peng, H. Wang and J. Yang, *J. Phys. Chem. C*, 2008, **112**, 6758–6763.
34 S. Fogden, R. Verdejo, B. Cottam and M. Shaffer, *Chem. Phys. Lett.*, 2008, **460**, 162–167.
35 K. S. Subrahmanyam, L. S. Panchakarla, A. Govindaraj and C. N. R. Rao, *J. Phys. Chem. C*, 2009, **113**, 4257–4259.